Chemistry & Biology, Vol. 12, 109–120, January, 2005, ©2005 Elsevier Ltd All rights reserved. DOI 10.1016/j.chembiol.2004.11.013

Single-Molecule Observation of the Catalytic Subunit of cAMP-Dependent Protein Kinase Binding to an Inhibitor Peptide

Hongzhi Xie,[1] Orit Braha,[2] Li-Qun Gu,[1] Stephen Cheley,[1] and Hagan Bayley[2,*]
[1]Department of Medical Biochemistry and Genetics
Texas A&M University System Health Science Center
440 Reynolds Medical Building
College Station, Texas 77843-1114
[2]Department of Chemistry
University of Oxford
Mansfield Road
Oxford OX1 3TA
United Kingdom

Summary

An engineered version of the staphylococcal α-hemolysin protein pore, bearing a peptide inhibitor near the entrance to the β barrel, interacts with the catalytic (C) subunit of cAMP-dependent protein kinase. By monitoring the ionic current through the pore, binding events are detected at the single-molecule level. The kinetic and thermodynamic constants governing the binding interaction and the synergistic effect of MgATP are comparable but not identical to the values in bulk solution. Further, the values are strongly dependent on the applied membrane potential. Additional exploration of these findings may lead to a better understanding of the properties of enzymes at the lipid/water interface. Despite the complications, we suggest that the engineered pore might be used as a sensor element to screen inhibitors that act at either the substrate or ATP binding sites of the C subunit.

Introduction

Protein kinases play a central role in a wide variety of normal and pathological processes [1]. The catalytic domains of these enzymes mediate the transfer of the γ-phosphate of ATP to cellular proteins involved in signaling, and the mechanism of this reaction has been studied in detail [1]. Because of the importance of protein kinases in disease, together with the availability of the human genome sequence, there has been considerable interest in high-throughput kinase assays. For example, almost all the kinases from the yeast *Saccharomyces cerevisiae* (numbering 122) were assayed in a disposable array of microwells with 15 different substrates [2], and new chip-based assays continue to be developed [3, 4]. There has also been renewed interest in protein kinase inhibitors, especially those that act at the ATP binding site, and several are now in the clinic or in trials [5, 6]. Despite these advances, procedures for screening inhibitors are still needed that would both increase throughput and, importantly, provide accurate kinetic constants for their association and dissociation. Here, we explore a means to assay protein kinases at the single-molecule level, which might eventually be developed into such an approach.

*Correspondence: hagan.bayley@chem.ox.ac.uk

To test our approach, we have used cyclic AMP-dependent protein kinase (PKA), which is the best-studied member of the kinase family [7, 8] and provides a prototype for its relatives, which number many hundreds in humans [9]. The PKA holoenzyme comprises two regulatory subunits (R) and two catalytic subunits (C). Upon activation by cAMP, the R subunits are released as a dimer with two molecules of cAMP bound to each. The C subunits dissociate as active monomers. Structures of the C subunit [10–13], including its complex with a fragment of the heat-stable protein kinase inhibitor [14], have been determined by X-ray crystallography.

In the present work, we have used stochastic sensing to examine the interaction of the C subunit with a fragment of the heat-stable inhibitor. The α-hemolysin (αHL) protein pore was used as the sensor element. In stochastic sensing, the ionic current driven through a single pore by a transbilayer potential is interrupted by the analyte, which is, in the present case, the C subunit. In this way, individual binding events are observed which reveal the concentration and identity of the analyte, the former from the frequency of occurrence of the binding events and the latter by the current signature, for example the dwell time of the analyte or the extent of current block caused by it. The approach has been used to monitor a wide variety of analytes [15], including proteins [16, 17].

α-Hemolysin is secreted by *Staphylococcus aureus* as a water-soluble monomeric polypeptide of 33.2 kDa. The assembled αHL pore is a mushroom-shaped heptamer [18] (Figure 1A). The opening of the pore in the mushroom cap, on the *cis* side of the bilayer, is ~30 Å in diameter. The cap contains a roughly spherical cavity with a diameter of ~45 Å. The stem is a β barrel that spans the lipid bilayer and averages ~20 Å in internal diameter. In one study, biotin was attached to one end of a poly(ethylene glycol) chain, which was attached covalently through the other end to a site within the lumen of the pore. In single-channel electrical recordings, the modified pore responded to various biotin binding proteins presented on the *cis* or *trans* side of the bilayer [16]. In a second study, a lectin presented from the *cis* side was shown to undergo monovalent and bivalent interactions with an αHL pore decorated on the cap with disaccharides [17]. In the present work, we have prepared an entirely different construct in which a single synthetic protein kinase inhibitor peptide (PKIP5-24) is tethered [16, 19, 20] at the narrow *trans* entrance of the pore with a flexible tetra(ethylene glycol) (TEG) linker. Binding of the C subunit to the tethered peptide causes a partial block of the single-channel current, which allows the kinetics of the interaction to be monitored.

Results

Construction of an αHL Pore with a Covalently Attached Protein Kinase Inhibitor Peptide, PKIP5-24

The peptide comprising amino acid residues 5–24 of the heat-stable protein kinase inhibitor (PKIP5-24) has

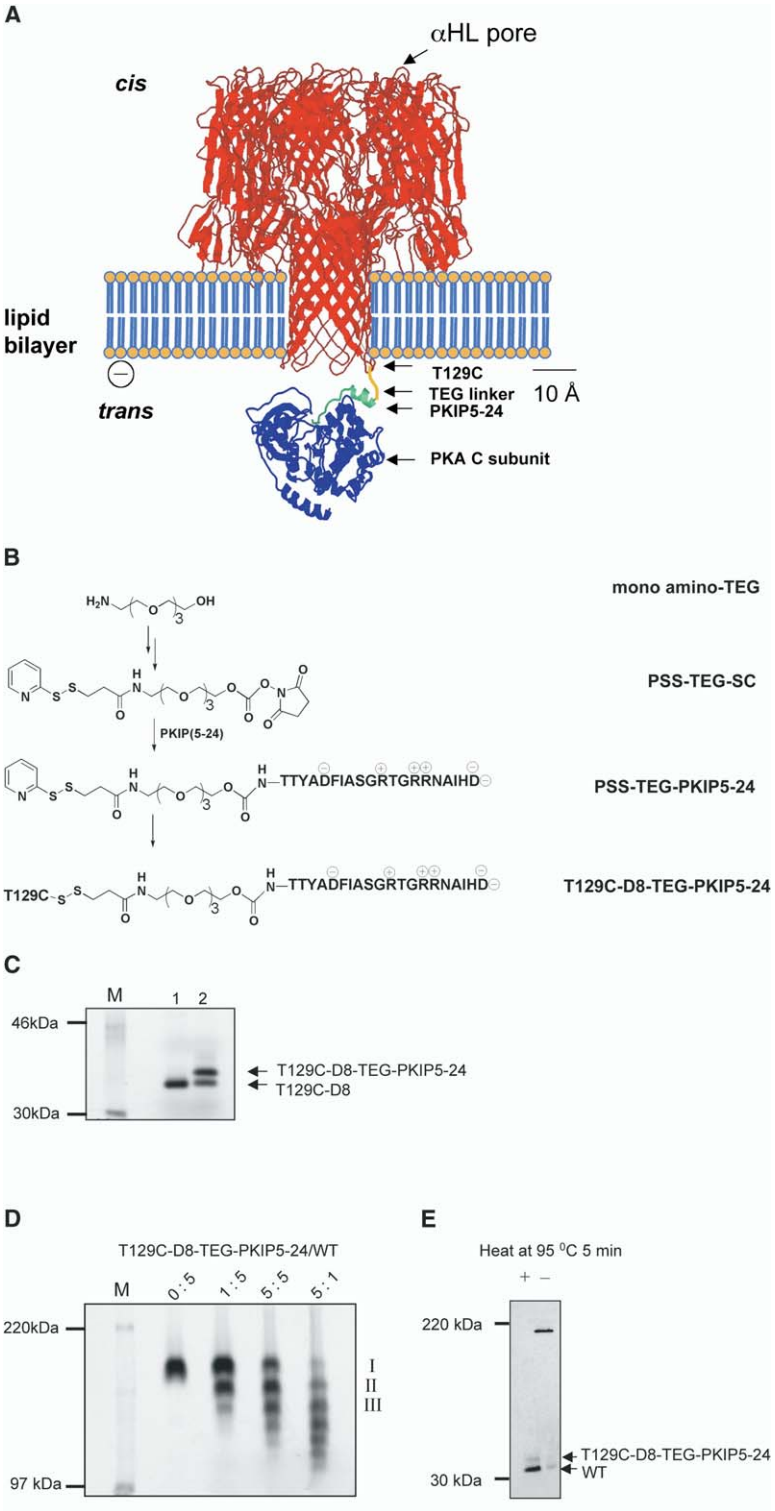

Figure 1. Preparation of an αHL Pore with a Single Covalently Attached Protein Kinase Inhibitor Peptide near the *trans* Entrance, the PKIP-Pore

(A) Molecular model of the PKIP-pore bound to the catalytic subunit of cAMP-dependent protein kinase. The heteroheptameric αHL pore contains one subunit modified with PKIP5-24 and six unmodified subunits. The N terminus of PKIP5-24 is tethered to a Cys residue at position 129 through a disulfide bond and a short flexible tetra(ethylene glycol) (TEG) linker. (B) Synthetic route to the modified αHL subunit. (C) Electrophoretic analysis of the modified αHL subunit. An autoradiograph of a 12% SDS-polyacrylamide gel is shown. Lane 1: unmodified T129C-D8 monomer; lane 2: the modified monomer T129C-D8-TEG-PKIP5-24. The positions of two molecular weight markers are indicated. The loading buffer contained no reducing agent. (D) Assembly of the PKIP-pore. An autoradiograph of a 5% SDS-polyacrylamide gel is shown containing heteroheptamers formed by the assembly of mixtures of T129C-D8-TEG-PKIP5-24 monomer and wild-type αHL monomer (WT) in different ratios (0:5, 1:5, 5:5, 5:1) on rabbit erythrocyte membranes. The bands are identified as follows: I, WT_7; II, $(T129C\text{-}D8\text{-}TEG\text{-}PKIP5\text{-}24)_1WT_6$; III, $(T129C\text{-}D8\text{-}TEG\text{-}PKIP5\text{-}24)_2WT_5$. The differences in mobility are caused by the numbers of D8 tails in each heptamer. The positions of two molecular weight markers are indicated. (E) Purity of the $(T129C\text{-}D8\text{-}TEG\text{-}PKIP5\text{-}24)_1WT_6$ heteroheptamer. Material eluted from a preparative gel was rerun in an analytical 12.5% SDS-polyacrylamide gel. The unheated sample (–) contained a single band of high mass. The heated sample (+) contained two low-mass bands representing the WT and T129C-D8-TEG-PKIP5-24 subunits.

nanomolar affinity for the C subunit of PKA [14, 21–25]. We constructed an αHL pore carrying a single PKIP5-24 at the *trans* mouth of the β barrel (Figure 1A). The derivatized pore comprised one subunit covalently modified with the peptide and six wild-type (WT) subunits. The modified subunit was prepared by attaching PKIP5-24 through a linker to a cysteine residue at position 129 (Figure 1B).

The PKIP5-24 conjugate required for derivatizing the protein was prepared beginning with the linker tetra (ethylene glycol) in which one of the terminal hydroxyls had been converted to an amino group (mono-amino-

TEG). The linker was heterobifunctionalized in two steps to form PSS-TEG-SC (Figure 1B). PSS-TEG-SC contains an S-pyridyl group at the amino end and an N-hydroxysuccinimidyl carbonate group at the hydroxyl end. The N terminus of PKIP5-24 was coupled to PSS-TEG-SC to form a peptide conjugate (PSS-TEG-PKIP5-24) with a carbamate linkage. PSS-TEG-PKIP5-24 was purified by reverse-phase HPLC and identified by MALDI-MS.

The αHL polypeptide (T129C-D8) required for chemical modification with PSS-TEG-PKIP5-24 contained a single cysteine at position 129 (Thr→Cys) and eight aspartate residues at the C terminus (D8 tail), and was prepared by in vitro transcription and translation (IVTT). The D8 tail was needed for the separation of heteromeric pores containing various combinations of WT and modified subunits [26]. PSS-TEG-PKIP5-24 reacted with the cysteine of T129C-D8 through the S-pyridyl disulfide to form T129C-D8-TEG-PKIP5-24 (Figure 1B). The extent of modification of T129C-D8 could be judged from the relative intensities of the T129C-D8 and T129C-D8-TEG-PKIP5-24 bands in an SDS-polyacrylamide gel and ranged from 65% to 70% (Figure 1C). Unpurified T129C-D8-TEG-PKIP5-24 was then mixed with the WT-αHL monomer, also prepared by IVTT, in various ratios and allowed to assemble on rabbit blood cell membranes to form a mixture of heteroheptamers as visualized by SDS-polyacrylamide gel electrophoresis (Figure 1D). The heteroheptamer containing a single copy of PKIP5-24, T129C-D8-TEG-PKIP5-24$_1$WT$_6$, was obtained by preparative electrophoresis. When the product, T129C-D8-TEG-PKIP5-24$_1$WT$_6$, was rerun on a gel, a single high-mass band was observed (Figure 1E), which upon heating dissociated into WT and T129C-D8-TEG-PKIP5-24 subunits in a ratio of 6.8:1, which is close to the desired value of 6.0:1 (Figure 1E). The modified subunits appear to become enriched in the assembled pore, based on the extent of modification of the T129C-D8 monomer (Figure 1C).

Interaction of the C Subunit of PKA with the PKIP-Pore

Single-channel current recording in planar lipid bilayers was used to investigate the interaction of the modified αHL pore T129C-D8-TEG-PKIP5-24$_1$WT$_6$ (PKIP-pore) with the ~40 kDa C subunit of PKA. The PKIP-pore was added to the *cis* chamber of the apparatus. Based on the crystal structure of the αHL heptamer [18], position 129, which is located at the tip of the transmembrane stem domain, should be exposed to bulk solution in the *trans* chamber provided that the preassembled pore with the attached peptide is able to insert normally through the bilayer. Remarkably, it can, to judge from the fact that the C subunit binds to the PKIP peptide from the *trans* side (see below).

Single-channel current-voltage (I-V) curves of the PKIP-pore (Figure 2A) showed that it is similar in character to the WT homoheptameric αHL pore (WT$_7$). Because a few pores lacked an attached peptide, the C subunit was always added at the end of an experiment to ensure that a modified pore had been examined. Unitary conductance values in 300 mM KCl, 15 mM MOPS (pH 6.80, titrated with 0.1 M KOH) were: PKIP-pore, 324 ± 9 pS (n = 3); WT$_7$, 332 ± 10 pS (n = 3), over the linear range of –40 to +40 mV. When 150 nM wild-type C subunit of PKA was added to the *trans* chamber, binding events manifested in a partial channel block occurred at an applied potential of –80 mV, and were characterized by a mean lifetime of 5.2 ± 1.4 s (n = 5) and an interevent interval of 2.6 ± 0.4 s (n = 5) (Figures 2B and 2E). The extent of the block was 88 ± 2%. Interestingly, no binding events were seen at positive applied potentials. Several experiments were performed to confirm that the blockades arise from the interaction of the C subunit with the tethered PKIP. When denatured C subunit (heated at 95°C for 5 min; Figure 2C) or bovine serum albumin (Figure 2D) was added to the *trans* side of the bilayer, no blockades occurred at a negative applied potential. The PKIP-pore remained open in the presence of the C subunit on the *cis* side of the bilayer at positive or negative potentials. There were also no blockades when 450 nM C subunit was added to the *trans* side of a bilayer containing WT$_7$ pores (data not shown).

The effect of free PKIP5-24 peptide on the interaction of the C subunit with the PKIP-pore was examined (Figure 2F). Free PKIP led to an increase in the interevent interval (τ_{on}) with no effect on the blockade lifetime (τ_{off}) (with free PKIP, τ_{off} = 6.0 ± 0.2 s [n = 3]; without free PKIP, τ_{off} = 5.2 ± 1.4 s [n = 5]). For example, in the presence of 2 μM PKIP5-24, τ_{on} increased from 3.5 ± 1.1 s to 250 ± 56 s (n = 3). Events of a much shorter lifetime (<1 ms) also appeared in the presence of free PKIP5-24, in the presence (Figure 2F) or absence of C subunit, which we ascribe to an interaction of the free peptide with the pore.

Kinetics of Block of the PKIP-Pore with C Subunit from Single-Channel Current Recording

Single-channel current recording was used to measure the association and dissociation rate constants for C subunits with the PKIP-pore. The binding events (current blockades) were characterized by the mean interevent interval (τ_{on}) and the mean event lifetime (τ_{off}) obtained from single exponential fits to lifetime histograms (not shown). The values of τ_{on} and τ_{off} were used to calculate the association ($k_{on} = 1/(\tau_{on} \cdot [C])$ and dissociation ($k_{off} = 1/\tau_{off}$) rate constants [27, 28]. A plot of $1/\tau_{on}$ versus the concentration of C subunit, [C], was linear, suggesting that the interaction of the PKIP-pore with the C subunit is bimolecular, as expected. In 300 mM KCl, 15 mM MOPS (pH 6.80), at an applied potential of –80 mV, $k_{on} = 2.5 \pm 0.5 \times 10^6$ M^{-1} s^{-1}, $k_{off} = 0.19 \pm 0.05$ s^{-1}, and $K_d = 7.6 \pm 1.4 \times 10^{-8}$ M (n = 6).

Kinetics of Block of the PKIP-Pore with C Subunit from Macroscopic Current Recording

Macroscopic (multichannel) current recording was also used to measure the kinetics of binding of the C subunit to the PKIP-pore. In single-channel recordings, we found that the C subunit did not produce current blockades at positive applied potentials. Therefore, the kinetics of C subunit binding from the *trans* side of the bilayer could be determined after a step in applied potential from +100 mV to –100 mV (Figures 3A and 3B). After the step, the current showed an exponential

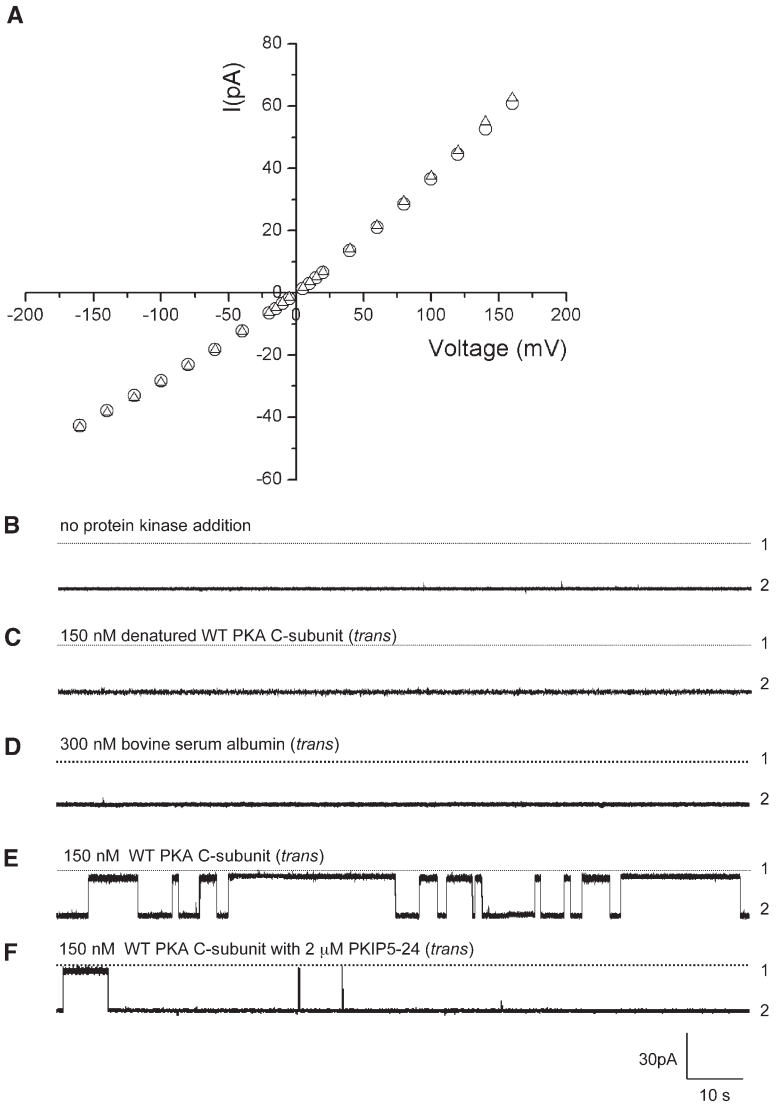

Figure 2. Detection of Individual Binding Events of the C Subunit to the PKIP-Pore

The PKIP-pore was introduced from the *cis* chamber. Both chambers contained 300 mM KCl, with 15 mM MOPS titrated with KOH (pH 6.80), at 25 ± 1°C. (A) Single-channel current-voltage (I-V) relationships. PKIP-pore (○); WT_7 pore (△). In (B)–(F), currents through single PKIP-pores at –80 mV are shown with various additions to the *trans* chamber. (B) No additions. (C) 150 nM denatured wild-type C subunit (heated at 95°C for 5 min). (D) 300 nM bovine serum albumin. (E) 150 nM wild-type C subunit. (F) 150 nM wild-type C subunit and 2 μM PKIP5-24 peptide. Level 1, zero current; level 2, free PKIP-pores. Because a few pores contained no attached PKIP peptide, the pores in (C) and (D) were tested by the subsequent addition of C subunit. The appearance of binding events showed that the pores indeed carried tethered peptides.

decay (Figure 3B) that was more rapid at more negative potentials, within the tested voltage range of –70 to –120 mV (Figure 3C), indicating that C subunits bind more quickly to PKIP at higher applied negative potentials. Macroscopic current decays were measured in triplicate in the presence of seven different concentrations of C subunit at various applied negative potentials (–70, –80, –90, –100, –120 mV). Values of $k_{on\text{-}v}$ and $k_{off\text{-}v}$ were then obtained from Equation 1.

$$k_{off-v} = P_v(\infty) / \tau_v \text{ and } (1 - P_v(\infty)) / \tau_v = k_{on-v} \cdot [E], \quad (1)$$

where $P_v(\infty)$ is the equilibrium open probability at voltage V and τ is the current decay constant. $P_v(\infty)$ and τ were obtained by fitting the multichannel current decay to Equation 2:

$$I_v(t) = I_v(0) \cdot [P_v(\infty) + (1 - P_v(\infty)) \cdot e^{-t/\tau}], \quad (2)$$

where $I_v(0)$ and $I_v(t)$ are the macroscopic currents at t = 0 and t, respectively, after a small correction for the presence of unmodified pores (for details, see Supplemental Data). At all applied potentials, $(1 - P(\infty))/\tau_v$ showed a linear relationship with the concentration of C subunit (Figure 4A), reinforcing the idea that the interaction of C with PKIP can be described as a simple bimolecular process (see Supplemental Data).

The k_{off} and k_{on} values were both voltage dependent. As the applied negative potential decreased from –120 to –70 mV, k_{off} was reduced by ~17-fold (from 1.5 ± 0.3 s^{-1} to 0.084 ± 0.031 s^{-1}; Figure 4B), and the value of k_{on} was reduced by almost 120-fold (from 7.5 ± 0.2 × 10^7 M^{-1} s^{-1} to 6.1 ± 0.7 × 10^5 M^{-1} s^{-1}; Figure 4C). The equilibrium dissociation constant ($K_d = k_{off}/k_{on}$) increased about 7-fold with decreasing applied negative potential (from 2.0 ± 0.3 × 10^{-8} M at –120 mV to 14 ± 1 × 10^{-8} M at –70 mV; Figure 4D). The kinetic data measured by macroscopic current recording are consistent with those measured by single-channel recording: at –80 mV, k_{on} = 8.3 ± 1.8 × 10^5 M^{-1} s^{-1} (n = 3; single-channel, 2.6 ± 0.4 × 10^6 M^{-1} s^{-1}); k_{off} = 0.10 ± 0.02 s^{-1}

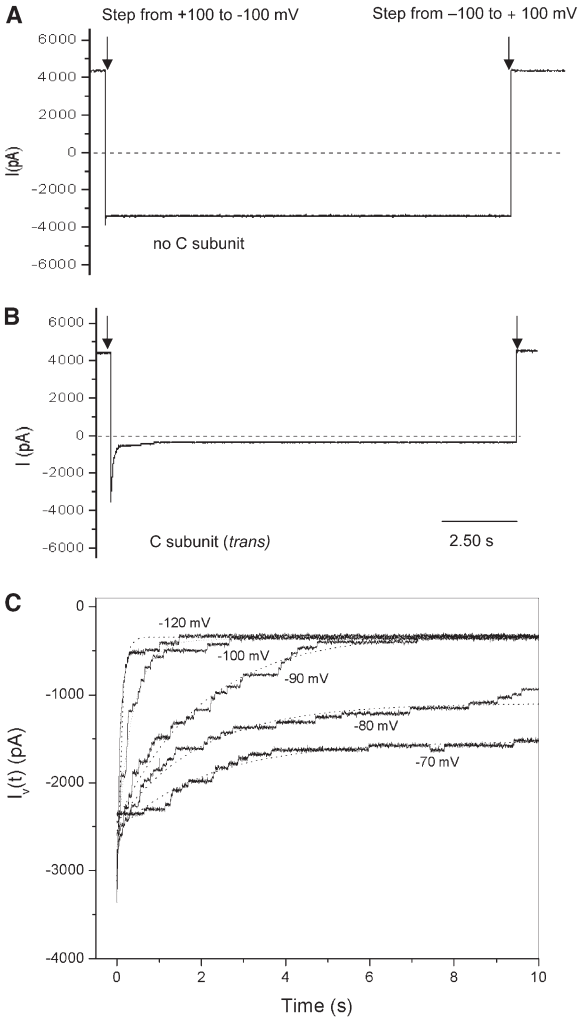

Figure 3. Macroscopic (Multichannel) Current Recordings of the Response of the PKIP-Pore to a Voltage Step in the Presence of C Subunit

During the recording, the applied potential was stepped from +100 mV to –100 mV as indicated. The buffer in both chambers was 300 mM KCl, 15 mM MOPS titrated with KOH (pH 6.80). (A) Current recording during voltage step in the absence of C subunit. (B) Current recording during voltage step in the presence of 180 nM C subunit in the *trans* chamber. (C) Kinetics of the drop in the macroscopic current in the presence of C subunit (100 nM, *trans*) after steps from +100 mV to various negative potentials, as indicated. The curves show single exponential fits with relaxation times: τ = 0.16 s (–120 mV); τ = 0.58 s (–100 mV); τ = 1.5 s (–90 mV); τ = 3.4 s (–80 mV); τ = 6.9 s (–70 mV).

(n = 3; single-channel, k_{off} = 0.19 ± 0.05 s^{-1}); K_d = 8.3 ± 1.9 × 10^{-8} M (n = 3; single channel, K_d = 7.6 ± 1.4 × 10^{-8} M).

Affinity of the C Subunit for the PKIP-Pore in the Presence of MgATP

The effect of MgATP on the interaction of the C subunit with the PKIP-pore was investigated by single-channel current recording. The values of $1/\tau_{on}$ for C subunit binding increased with increasing MgATP concentration, while the values of $1/\tau_{off}$ decreased (Figure 5). The K_d value for the interaction of the C subunit with the PKIP-pore is 1.4 nM (at –80 mV) extrapolating to saturation of the kinase with MgATP (for details, see Supplemental Data), compared with 76 nM in the absence of ATP. The kinetic data for the interaction of the C subunit with the PKIP-pore measured under various conditions are summarized in Table 1, and compared with those reported in the literature.

Discussion

The present study was primarily designed as the initial step in obtaining a stochastic sensing device for protein kinases that might also be used to screen kinase inhibitors. This goal has been achieved, and with additional refinement, the engineered pore that we have devised might also be used for the quantitative examination of kinase-inhibitor interactions at the single-molecule level.

We have previously used engineered αHL pores to examine protein-ligand interactions. Because the proteins of interest are too large to enter the pore, binding sites for them cannot be built into the lumen as they have been in other examples of stochastic sensing [15]. Instead, binding events in the external medium must be transmitted to the interior of the pore or the protein must bind close enough to the entrance of the pore to affect its conductance. In an example of the first possibility, we attached a ligand (biotin) to the end of a 3400 Da poly(ethylene glycol) chain [16]. The other end of the polymer was anchored to residue 106 within the cap of the pore. In the absence of a biotin binding protein, movement of the polymer within the pore produced a "noisy" single-channel current. Upon binding streptavidin, or an anti-biotin antibody, the current became quiet. Analysis of the frequency of occurrence of the binding events represented by the quiet current allowed the concentration of the binding protein to be quantified. In an example of the second approach, disaccharides were attached through a short linker to a site near the *cis* entrance of the pore [17]. In this case, the single-channel current was quiet, and the binding of a lectin to either one or two of the disaccharides was manifested by a reduction in the current flowing through the pore. Again, analysis of the binding events allowed the concentration of the binding protein to be quantified.

The present work tests a third configuration, in which a peptide ligand is presented at the *trans* entrance of the pore. In this case, the binding of a protein kinase to the peptide is also manifested by a reduction in current. A heteromeric pore, PKIP-pore, was prepared, which contained a single copy of the protein kinase inhibitor peptide, PKIP5-24. The PKIP-pore inserted into a planar bilayer after introduction into the *cis* chamber of the apparatus at a concentration of 0.12 ng ml^{-1}. This is surprising, as the rather polar attached peptide must be transported through the lipid bilayer (the typical time for the appearance of a pore for WT_7 presented at 0.04 ng ml^{-1} was usually somewhat faster). Conceivably, the

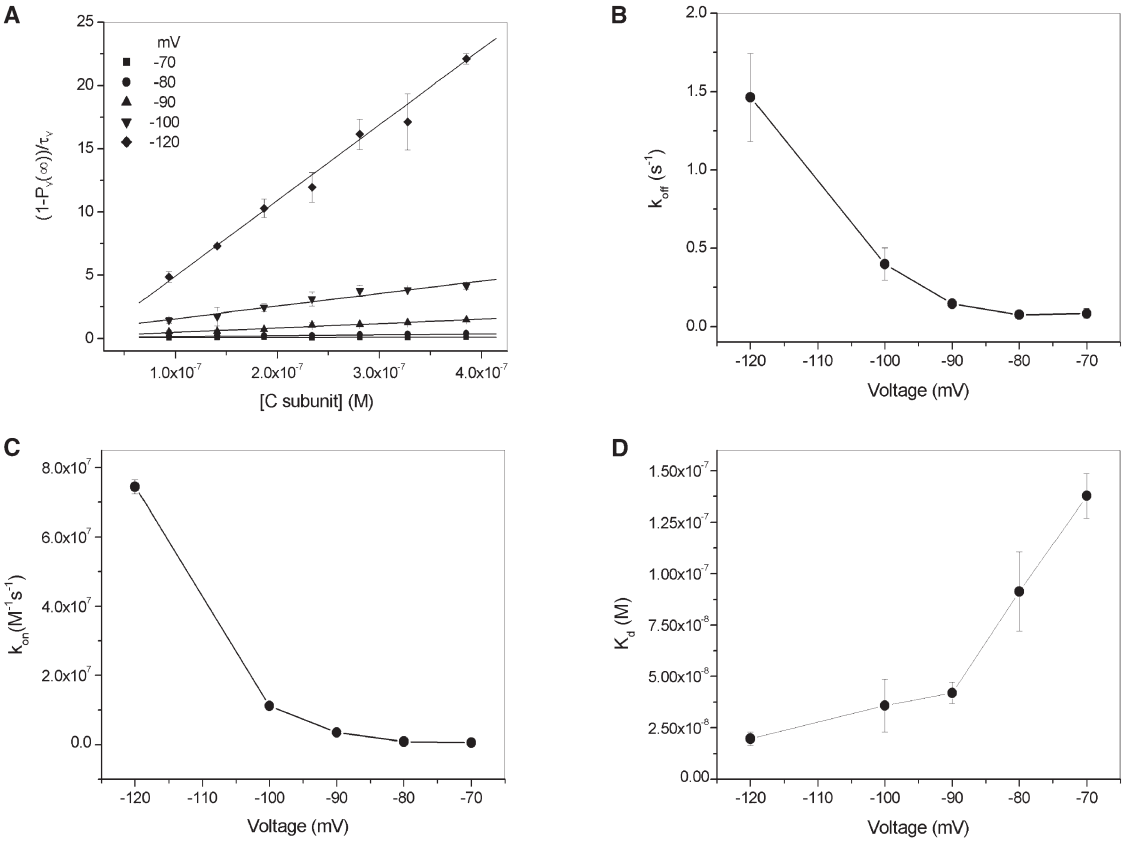

Figure 4. Kinetic Analysis of C Subunit Binding to the PKIP-Pore

(A) The dependence of $(1 - P_v(\infty))/\tau_v$ on the concentration of C subunit at various applied potentials, where $P_v(\infty)$ is the probability that the pore is unblocked by the C subunit. (B) The voltage dependence of the dissociation rate constant, k_{off}. (C) The voltage dependence of the association rate constant, k_{on}. (D) The voltage dependence of the equilibrium dissociation constant, K_d. The kinetic parameters were obtained from the current decay curves reflecting the response of the PKIP-pore to a voltage step in the presence of C subunit (Figure 3 and Supplemental Data). The data are the means ± SD of three experiments at various concentrations of C subunit.

peptide is concealed within the barrel of the pore, but current recordings (see below) suggest that, if this is the case, the barrel must become quickly unblocked after insertion. The PKIP-pore was isolated after electrophoresis in an SDS-polyacrylamide gel and was therefore likely to contain traces of SDS, which might facilitate insertion.

Single-channel current recordings of the WT αHL pore and the PKIP-pore provided I-V curves that were closely similar (Figure 2A). This suggests that the PKIP peptide has little interaction with the transmembrane β barrel. Nevertheless, at positive applied potentials, the peptide is unavailable for binding by the C subunit. Because the conductance values at these potentials are similar to those of the WT pore, the peptide cannot be rendered inaccessible by transport into the barrel. Perhaps it is sequestered against the surface of the lipid bilayer. At first sight, this seems unlikely, as the charge on the peptide is near neutral and the lipid bilayer is formed from phosphatidylcholine, which has a zwitterionic head group. However, when folded as an α helix, the peptide has a strong transhelix dipole and may move into the membrane surface as part of the capacitative charge at positive applied potentials and be released rather than reorient at negative potentials, because the negative face contains a high proportion of hydrophilic residues compared to the positive face. Residues 1–15 are helical in solution as determined by NMR [25] and an increase in helicity could occur at the membrane interface.

When measured at an intermediate applied potential of –80 mV, the association and dissociation rate constants, and the equilibrium dissociation constant, for the interaction of C with PKIP, obtained by current recording with the PKIP-pore, are similar to those in the literature (Table 1). The K_d for the C subunit in the presence of MgATP (Table 1) is also close to the value expected. However, the data suggest that the system must be examined more deeply, if kinetic and binding constants that reflect those in bulk solution are to be obtained. A major issue is the voltage dependence of both k_{on} and k_{off}. At potentials more negative than –90 mV, K_d (k_{off}/k_{on}) attains a constant value of $\sim 4.2 \times 10^{-8}$ M, suggesting that the variation in k_{on} in this range is compensated by the variation in k_{off}. The variation of the rate constants at potentials below –90 mV is likely to arise from a voltage-dependent change in the local environment near the membrane surface. A compen-

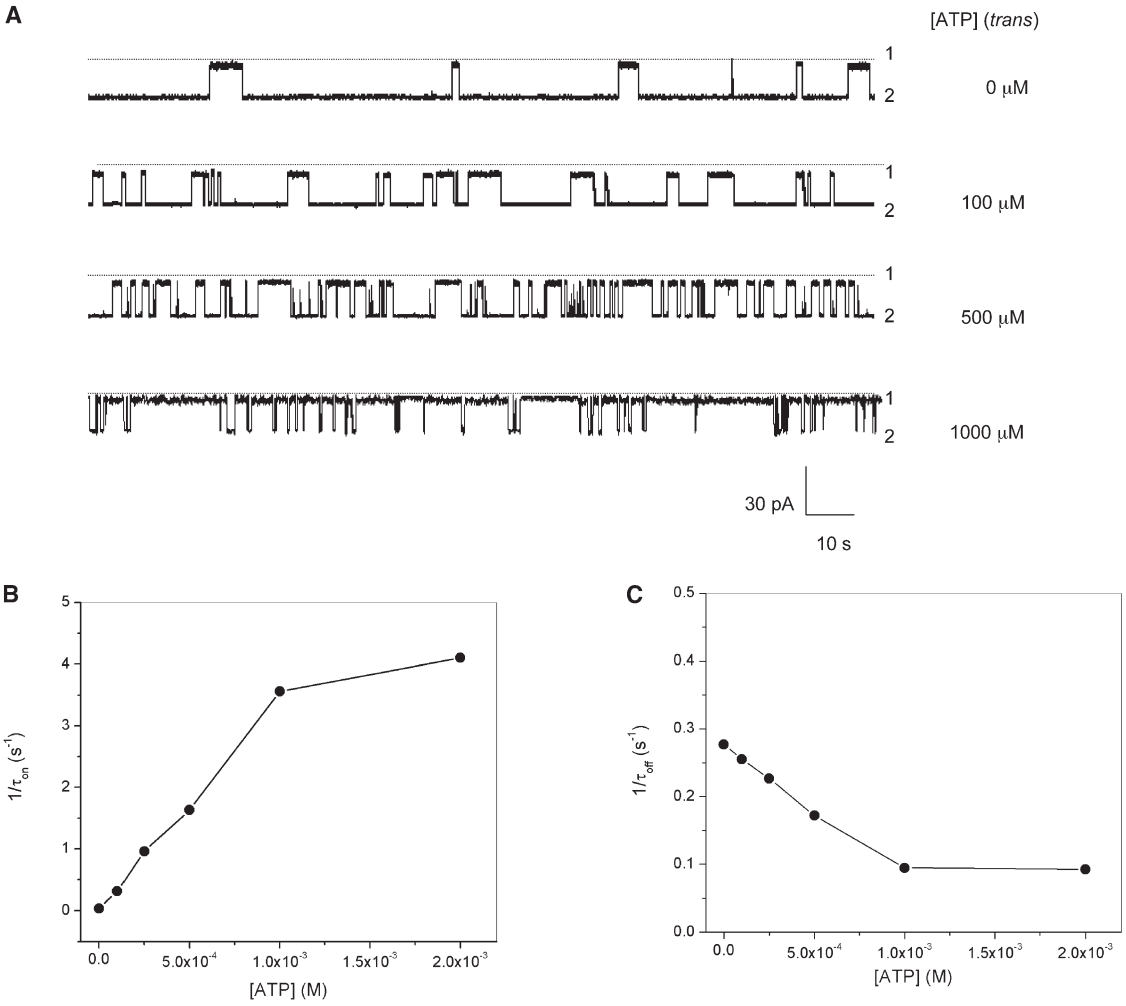

Figure 5. Effect of MgATP on the Binding of C Subunit to the PKIP-Pore

The PKIP-pore was introduced from the *cis* chamber, and the C subunit and MgATP from the *trans* chamber. Both chambers contained 300 mM KCl, with 15 mM MOPS titrated with KOH (pH 6.80), at 25 ± 1°C. Recordings were made at −80 mV. (A) Single-channel currents at various concentrations of ATP and 10 mM $MgCl_2$ in the presence of 100 nM C subunit. Level 1, zero current; level 2, free PKIP-pores. (B) Plot of $1/\tau_{on}$ versus the concentration of ATP. (C) Plot of $1/\tau_{off}$ versus the concentration of ATP.

sating effect would be expected if the barrier between the two states (bound/unbound) is lowered at high negative potentials. At negative potentials up to −90 mV, values of k_{on} are more strongly affected by the applied potential and it seems likely that this can be accounted for in part by the accessibility of the PKIP peptide attached to the pore, as discussed earlier. While the origin of the voltage dependence of binding requires further investigation, the K_d value for the C subunit and the PKIP-pore is at least in the correct range, and binding is stimulated, as expected, by MgATP [24, 29–31] and inhibited by free PKIP. Other issues include the salt concentration at which measurements are made. We used 300 mM KCl, as opposed to the more usual ~100 mM KCl, to improve the signal-to-noise ratio in our current recordings. In the absence of MgATP, the PKI·C subunit complex dissociates more readily in solution at even 250 mM KCl, but it is greatly stabilized by MgATP [24]. Given the excellent quality of our data, it should be possible to use lower salt concentrations in future experiments.

A deeper understanding of the system will be obtained by working with inhibitor peptides with different net charges and different linker lengths. It may also be possible to modulate the accessibility of the inhibitor peptide by altering the surface charge of the lipid bilayer. Nevertheless, it could prove difficult to achieve conditions that reflect bulk solution on the *trans* side of the bilayer. For example, if the ligand can be placed at a greater distance from the *trans* entrance, it is likely that binding of the C subunit will have a lesser effect on conductance, which would ultimately make the events more difficult to detect. In earlier work, we examined the interaction of various biotin binding proteins presented from the *cis* chamber with biotin attached to one end of a 3.4 kDa poly(ethylene glycol) chain. The other end of the chain was tethered covalently to a site within the lumen of the pore [16]. In this configuration,

Table 1. Kinetic Data for the Interaction of the PKIP-Pore with the C Subunit of Protein Kinase A Obtained by Single-Channel or Macroscopic Current Recording, Compared with Values from the Literature

	Method	k_{on} (M^{-1} s^{-1})	k_{off} (s^{-1})	K_d (nM)
This Work				
	Single-channel recording[a]			
PKIP-pore·C_α	–MgATP	$2.5 \pm 0.5 \times 10^6$	0.19 ± 0.05	76
	+MgATP	$7.0 \pm 0.6 \times 10^7$	0.10 ± 0.02	1.4
	Macroscopic recording[a]			
	–MgATP	$8.3 \pm 1.8 \times 10^5$	0.10 ± 0.02	83
From the Literature				
	Gel filtration			
PKI·C_α	–MgATP	—	—	2300
	+MgATP	—	—	0.5
	Surface plasmon resonance			
GST-PKI·C_α	–MgATP	—	—	
	+ MgATP	1.5×10^6	0.00076	0.5
	Kinase assay			
PKIP5-24·C_α	+ MgATP	—	—	2.3 (K_i)
PKI·C_α	+ MgATP	—	—	0.2 (K_i)

PKIP-pore represents the T129C-D8-TEG-PKIP5-24$_1$WT$_6$ pore used in this work. PKI·C_α is the complex of skeletal muscle heat-stable protein kinase inhibitor (PKI) with wild-type C subunit in the absence and presence of 100 μM ATP and 1 mM $MgCl_2$ [24]. GST-PKI·C_α is the complex of a GST-PKI fusion protein with wild-type recombinant C_α [52]; PKIP5-24·C_α is the complex of PKIP5-24 inhibitor peptide with wild-type C subunit [30].

[a] Single-channel and macroscopic recordings were carried out in 300 mM KCl, 15 mM MOPS (pH 6.80) at an applied potential of –80 mV. The C subunit was added to the *trans* chamber in the absence and presence of ATP with 10 mM $MgCl_2$. The kinetic constants were obtained as described in the text and Supplemental Data. The data are mean values ±SD measured in independent experiments (single-channel: n = 6; macroscopic: n = 3) with the C subunit at different concentrations. The apparent dissociation constants K_d were obtained from $K_d = k_{off}/k_{on}$, where the k_{off} and k_{on} are the dissociation rate and association rate constants, respectively.

the binding events most probably occurred at a significant distance from the membrane surface, as the cap domain of the pore provides a 5 nm "spacer" and the poly(ethylene glycol) when elongated is 27 nm in length. In this case, the association and dissociation rate constants, and the equilibrium dissociation constants, were similar to those observed by other techniques, but a more thorough investigation of the voltage dependence of binding is warranted in this case too.

Whether or not the conditions in bulk solution can be mimicked, it might be worth attempting to observe enzymatic turnover by attaching a substrate, rather than an inhibitor, to the αHL pore. Such an experiment would be done in the presence of a phosphatase and the state of the tethered substrate (unphosphorylated or phosphorylated) would be detected by the length of the dwell time with the kinase or phosphatase. For example, the unphosphorylated peptide would be expected to bind to the kinase for longer than the phosphorylated product [32]. Fluorescence and other optical techniques have been used to monitor enzyme turnover at the single-molecule level [33–35], but the present approach would have the advantage of not requiring substrates coupled to bulky fluorescent dyes [36, 37] or the application of force to monitor or slow down reactions [38].

Many enzymatic reactions occur on or near membrane surfaces. For example, several protein kinases are acylated with fatty acids and might phosphorylate local substrates during a transient association with the lipid bilayer [39–43]. In other cases, protein kinases are brought into the vicinity of the bilayer by anchoring proteins [44], and tyrosine kinases are inhibited by hyperpolarization of cells [45]. The functional properties of ion channels themselves can be altered by interactions with the membrane surface. For example, the inactivation of voltage-gated K channels is strongly affected by the present of phosphoinositides with negatively charged head groups [46]. The approach we are using might be used to examine the influence of the prevailing conditions, such as the applied potential or fixed surface charge, on the functional properties of proteins.

In terms of making a sensor for protein kinases or for assaying kinase inhibitors, perfect replication of the conditions in bulk solution is less important. In the present work, we have shown that we can detect an inhibitor that binds at the substrate site (PKIP itself; Figure 2E) and MgATP (Figure 5). Because most small-molecule inhibitors of protein kinases bind at the ATP site [6], it should be possible to examine this important group of therapeutic agents. For example, a gradient of a potential inhibitor could be allowed to flow through a *trans* chamber of reduced volume in the presence of fixed concentrations of a protein kinase and MgATP. In this way, the kinetics of the interaction and the K_i could be determined in a few minutes. Unless it were made parallel, the throughput would be lower than that of various chip-based procedures [2, 3, 47, 48], but the ability to assay in real time and to determine the kinetics of inhibition as well as the K_i value would be an important

advantage, allowing the rapid acquisition of detailed information about the interaction of potential therapeutic agents with a target protein.

Significance

Protein engineering has been used to create a pore to which a single copy of a protein kinase inhibitor peptide (PKIP5-24) is tethered. By monitoring the current passing through an individual pore, the interaction of the substrate binding site of the C subunit of protein kinase A with the peptide can be observed at the single-molecule level. The engineered pore therefore has the potential to act as a sensing element for the C subunit in a stochastic sensor. A sensor of this kind might be used to screen a set of expressed protein kinases [2] for interactions with peptides (or peptidomimetics). Inhibitors designed to bind at a kinase substrate site could be examined in a competition assay. MgATP modulates the binding activity, and therefore inhibitors that interact with the ATP binding site might also be assayed. In a parallel format, numerous kinases could be assayed with numerous potential inhibitors. Although chip formats may have a higher throughput, the stochastic sensing approach provides additional information, such as the kinetics of the interaction between the kinase and an inhibitor. The approach we have developed might also be used to examine the functional properties of enzymes located at the lipid/water interface.

Experimental Procedures

General

The 20-amino acid protein kinase inhibitor (5-24) peptide, TTYADFIASGRTGRRNAIHD, was purchased from Synpep (Dublin, CA). The peptide was 95% pure as determined by HPLC. Bovine serum albumin (>99%), magnesium chloride (99%), and adenosine 5′-triphosphate disodium salt (99%) were purchased from Sigma (St. Louis, MO). Tetra(ethylene glycol) (99%), p-toluenesulfonyl chloride (98%), potassium phthalimide (98%), hydrazine monohydrate (98%), 3-mercaptopropionic acid (>99%), and N-hydroxysuccinimide (97%) were purchased from Aldrich (Milwaukee, WI). 2,2′-dithiodipyridine (97%), N,N′-dicyclohexylcarbodiimide (DCCD; 99%), and di(N-succinimidyl) carbonate (97%) were from Fluka. Anhydrous solvents were from Aldrich and used without further treatment. ^{1}H NMR spectra were recorded on a Varian Mercury 300 spectrometer. Mass spectra were obtained with a PerSeptive Biosystems Voyager MALDI-TOF mass spectrometer.

Synthesis

The synthetic route to the tetra(ethylene glycol)-functionalized linker is shown in Figure 6.

p-Toluenesulfonic Acid 2-[2-[2-Hydroxyethoxy] ethoxy]ethoxy Ethyl Ester (2)

To a solution of tetra(ethylene glycol) (20 g, 0.116 mol) and anhydrous pyridine (8 ml, 0.1 mol) in 40 ml of anhydrous dichloromethane was added, dropwise, a solution of p-toluenesulfonyl chloride (3.82 g, 0.02 mol) in 20 ml of dichloromethane. The reaction mixture was stirred at room temperature under argon. The formation of product was monitored by silica gel TLC with dichloromethane/methanol (10/1; R_f = 0.42). After 20 hr, the solution was evaporated under reduced pressure. The residue was dissolved in dichloromethane, loaded onto a silica gel column, and eluted with dichloromethane/methanol (50/1–20/1). The pure product was obtained as a colorless oil (5.15 g, 75% yield based on p-toluenesulfonyl chloride). ^{1}H NMR (300 MHz, $CDCl_3$) δ 2.45 (s, 3H), 2.60 (br, s, 1H), 3.52–3.67 (m, 14H), 4.12 (t, J = 4.8 Hz, 2H), 7.30–7.33 (d, J = 8.0 Hz, 2H), 7.75–7.78 (d, J = 8.4 Hz, 2H).

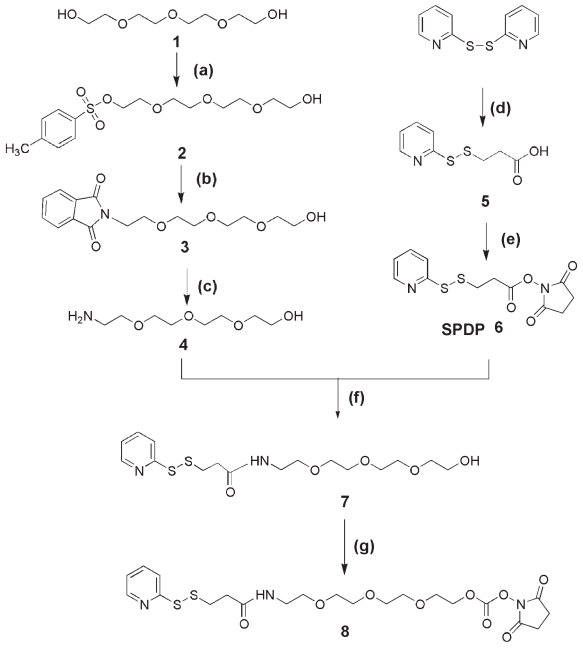

Figure 6. Synthesis of 2-[2-(2-N-Succinimidyl Carboxyethoxy)ethoxy] ethoxy-[3′-(2′-Pyridyldithio)-Propionyl] Ethyl Amide (**8**)

Reagents and conditions: (a) p-toluenesulfonyl chloride, CH_2Cl_2, pyridine, RT 20 hr, 75%; (b) potassium phthalimide, DMF, reflux overnight, 58%; (c) $NH_2NH_2.H_2O$, EtOH, 70°C overnight, not isolated; (d) 3-mercaptopropionic acid, EtOH, RT 4 hr, 84%; (e) N-hydroxysuccinimide, DCCD, CH_2Cl_2, RT overnight, 95%; (f) CH_3CN, RT 4 hr, not isolated; (g) di-N-succimidyl carbonate, CH_3CN, RT overnight, 50% yield from **3**.

2-[2-[2-Hydroxyethoxy]ethoxy]ethoxy Ethyl Phthalimide (3)

A mixture of tetra(ethylene glycol) monotosylate **2** (2.25 g, 6.4 mmol) and potassium phthalimide (1.43 g, 7.68 mmol) in dry DMF (15 ml) was degassed and refluxed for 10 hr under argon protection. Silica gel TLC indicated the formation a new less polar compound (dichloromethane/methanol 10/1; R_f 0.51). The solvent was evaporated under reduced pressure at 60°C. The residue was suspended in methanol (2 ml), loaded onto a silica gel column, and eluted with hexane/ethyl acetate (1/1) to yield the product as an orange oil (1.2 g, 57%). ^{1}H NMR (300 MHz, $CDCl_3$) 2.60 (br, s, 1H), 3.52–3.72 (m, 12H), 3.70–3.74 (m, J = 6.00 Hz, 2H), 3.86–3.89 (t, J = 5.40 Hz, 2H), 7.68–7.71 (dd, J = 3.3 Hz, 2H), 7.80–7.83 (dd, J = 3.3 Hz, 2H).

2-[2-[2-Hydroxyethoxy]ethoxy]ethoxy Ethylamine (4)

A mixture of tetra(ethylene glycol) monophthalimide **3** (0.4 g, 1.2 mmol) and hydrazine monohydrate (90 mg, 1.8 mmol) in absolute ethanol (2 ml) was degassed and then heated with stirring at 60°C overnight. After removing a precipitate by filtration, the solution was evaporated to dryness under reduced pressure. The residue was taken up in dichloromethane and filtered to remove undissolved material. The solvent was evaporated and the residue exposed to high vacuum to yield a colorless oil that was used for the next step without further purification. ^{1}H NMR (300 MHz, $CDCl_3$) 2.80 (t, J = 4.2 Hz, 2H, CH_2N), 3.38–3.75 (m, 15H, CH_2OCH_2, $HOCH_2$).

N-Succinimidyl 3-(2-Pyridyldithio)-Propionate (SPDP, 6)

SPDP was synthesized and purified by modifying a literature method [49]. A much better yield was obtained in both steps by using lower reactant concentrations.

To a solution of dithiodipyridine (3.75 g, 17 mmol) in ethanol (30 ml) containing glacial acid (0.4 ml), a solution of 3-mercaptopropionic acid (0.9 g, 8.5 mmol) in ethanol (20 ml) was added dropwise with vigorous stirring over a period of 15–20 min. After 2 hr, the yellow solution was evaporated under reduced pressure to obtain a yellow oil. This crude product was dissolved in dichloromethane/ethanol (4/1, 5 ml) and applied to a basic Al_2O_3 column. The column was washed with dichloromethane/ethanol (3/2) to elute starting materials and byproducts, and then **5** was eluted with dichloromethane/ethanol (3/2) containing 4% acetic acid. The solvents were removed under high vacuum to produce a colorless viscous oil (1.54 g, 84%). ^{1}H NMR (300 MHz, CD_3OD), δ 2.68–2.73 (t, J = 7.20 Hz, 2H), 3.02–3.06 (t, J = 6.90 Hz, 2H), 7.20–7.25 (t, J = 5.0 Hz, 1H), 7.78–7.87 (t, J = 7.2 Hz, 2H), 8.39–8.41 (d, J = 4.8 Hz, 1H).

A mixture of compound **5** (1.44 g, 6.7 mmol), N-hydroxysuccinimide (0.86 g, 7.4 mmol), and dicyclohexylcarbodiimide (1.53 g, 7.4 mmol) in anhydrous dichloromethane (40 ml) was stirred at room temperature for 3–4 hr. The formation of product was followed by silica gel TLC using dichloromethane/methanol (10/1) as eluant (R_f = 0.68). After filtration of a precipitate, the solution was evaporated to dryness under reduced pressure. The residue was purified on a silica gel column by using dichloromethane/methanol (50/1) as the eluant to obtain a viscous colorless oil, which became a white solid at 4°C overnight (2.04 g, 95%). ^{1}H NMR (300 MHz, $CDCl_3$), δ 2.84 (s, 4H), 3.04–3.16 (ddd, J = 5.7 Hz, 4H), 7.09–7.14 (t, J = 4.5 Hz, 1H), 7.65–7.68 (t, J = 5.4 Hz, 2H), 8.48–8.51 (d, J = 5.4 Hz, 1H).

2-[2-(2-N-Succinimidyl Carboxyethoxy)ethoxy]ethoxy-[3′-(2′-Pyridyldithio)-Propionyl] Ethyl Amide (8)

A mixture of tetra(ethylene glycol) mono-amine **4** (1.2 mmol) and SPDP **6** (0.42 g, 1.329 mmol) in dry acetonitrile (3 ml) was stirred for 5 hr at room temperature. The solvent was evaporated under reduced pressure and the crude product **7** was dried overnight under vacuum in the presence of P_2O_5. Without purification, **7** was dissolved in dry acetonitrile, mixed with di-N-succinimidyl carbonate (0.23 g, 0.9 mmol) and pyridine (0.2 ml, 2.60 mmol), and stirred overnight at room temperature under argon protection. The solvent was evaporated under reduced pressure and the residue was purified on a silica gel column eluted with dichloromethane/methanol (30/1) yielding 330 mg of product as a slightly yellow oil (50% overall yield). ^{1}H NMR (300 MHz, $CDCl_3$), δ2.61–2.66 (t, J = 7.0 Hz, 2H), 2.76 (s, 4H), 3.07–3.12 (t, J = 6.9 Hz, 2H), 3.48–3.50 (dd, J = 5.1 Hz, 2H), 3.58–3.60 (dd, J = 4.0 Hz, 2H), 3.64–3.71 (m, 8H), 3.78–3.81 (t, J = 4.8 Hz, 2H), 4.46–4.49 (t, J = 4.5 Hz, 2H), 7.11–7.14 (m, 1H), 7.66–7.13 (t, J = 6.0 Hz, 2H), 8.49–8.52 (J = 6.0 Hz, 1H). m/z (ESI): 532.1, $C_{21}H_{29}N_3O_9S_2$ requires 531.60.

PKIP5-24 Conjugate (9)

To a solution of PKIP5-24 peptide (Thr-Thr-Tyr-Ala-Asp-Phe-Ile-Ala-Ser-Gly-Arg-Thr-Gly-Arg-Arg-Asn-Ala-Ile-His-Asp; 2.2 mg, 1 μmol) in DMSO (100 μl) were added 20 μl of compound **8** in DMSO (0.1 M) and 6 μl of triethylamine in DMSO (1 M). The mixture was incubated overnight at 37°C under argon. The N terminus of the peptide reacts with **8** to form a carbamate bond with the functionalized tetra (ethylene glycol) linker (Figure 1B). The solvent was evaporated under high vacuum, yielding a glassy solid. This material was separated by HPLC on a Vydac C_{18} reverse-phase column (4.6 × 250 mm) by using a linear gradient formed with solvent A (0.05% trifluoroacetic acid in water) and solvent B (0.05% trifluoroacetic acid in 90% acetonitrile/10% water). The gradient ran from 5% to 40% solvent B over 40 min at a flow rate of 1.0 ml min^{-1}. Two major peaks were observed at 280 nm: the starting peptide PKIP5-24 (t = 23.3 min) and the desired, less polar product (t = 28.1 min). The latter fractions were freeze dried giving a white powder (yield, 50%). MALDI-MS $(M)^+$: 2640.31 found, 2639.84 calculated. A peak at $[M-110]^+$: 2531.07 was also observed that probably arises from cleavage of the 2-thiopyridone group in the laser beam. Purified **9** (97% purity by rerunning on HPLC) was dissolved in water at a concentration of 5 mM and stored at –20°C before use.

Proteins

The T129C-D8 gene was made by in vivo recombination using PCR products derived from two plasmids, pT7-αHL-T129C and pT7-αHL-WTD8. The latter contains a wild-type gene with eight additional aspartate residues at the C terminus. The forward primer for pT7-αHL-WTD8 was SC279: 5′-GGGAAAAAGAAGAAATGACAAA TGATGACGATGATGACGACGATGATTGATAAGCTT-3′. The reverse primer for pT7-αHL-T129C was SC280: 5′-AAGCTTATCAATCAT CGTCGTCATCATCGTCATCATTTGTCATTTCTTCTTTTTCCC-3′. The reverse primer used for PCR from pT7-αHL-WTD8 was SC47: 5′-CAGAAGTGGTCCTGCAACTTTAT-3′, while the forward mutagenic primer for PCR from pT7-αHL-T129C was SC46: 5′-ATAAAG TTGCAGGACCACTTCTG-3′. The negative charge of the "D8 tail" of the T129C-D8 protein was expected to change the electrophoretic mobility of the assembled pore allowing the separation of heteroheptamers [26]. WT and T129C-D8 αHL proteins were synthesized by using an in vitro transcription and translation (IVTT) kit (Promega, Madison, WI). In general, an IVTT reaction (25 μl) was carried out by mixing plasmid DNA (4 μl, 400 ng μl^{-1}), an S30 mix without amino acids (10 μl), a complete amino acid mix (2.5 μl, a mixture of the minus-leucine [L995B] and minus-cysteine [L447A] amino acid mixes), [^{35}S]methionine (1 μl; Amersham Pharmacia Biotech, Piscataway, NJ; 1,200 Ci/mmol, 10 mCi ml^{-1}), and an *E. coli* S30 extract (7.5 μl, T7 S30, L114A). After 1 hr at 37°C, the mixture was centrifuged for 2 min at 10,000 × g. The protein in the supernatant was separated from thiols and other low-molecular mass material with a G-25 Gel Filtration Micro SpinColumn (Harvard Apparatus, Holliston, MA), that had been equilibrated in 10 mM MOPS (pH 7.4) titrated with KOH.

Protein Modification

The T129C-D8 protein monomer (5 μl) was diluted with a buffer (5 μl) containing 10 mM MOPS (pH 6.80), 0.5 mM EDTA, and then mixed with the PKIP conjugate **9** (5 μl, 5 mM). The reaction was monitored by electrophoresis in a 12% SDS-polyacrylamide gel, followed by autoradiography of the dried gel. After 1 hr at room temperature, about 70% of the T129C-D8 monomer had been modified by **9** conjugate to form T129C-D8-TEG-PKIP5-24.

Protein Pores

T129C-D8-TEG-PKIP5-24 (6 μl, 3× diluted with 10 mM MOPS [pH 7.4] titrated with KOH, containing 150 mM NaCl) and wild-type αHL monomer (10 μl, prepared by IVTT and passed without dilution through a Sephadex G-25 spin column equilibrated in 10 mM MOPS [pH 7.4]) were mixed in various ratios. Pores were then allowed to assemble on rabbit erythrocyte membranes (5 μl, 4.0 mg/ml) for 1 hr at 37°C. The membranes were spun down and the supernatant was discarded. The membranes were then washed once using the same buffer. The pellets were then dissolved in sample buffer (10 μl of 10% glycerol, 2.3% SDS, 0.0625 M Tris.HCl [pH 7.5]) and loaded onto 5% SDS-polyacrylamide gels (35 cm long, 1.5 mm thick), which were run for 18 hr at 50 V. The gels were dried onto Whatman 3MM paper under vacuum at 50°C for 3 hr, and the protein bands were located by autoradiography. The pore with a single tethered PKIP5-24 was estimated to be ~40% of the total protein in the mixture of pores, formed from a mixture of monomers containing T129C-D8-TEG-PKIP5-24 and wild-type in a ratio of 1:5 (Figures 1C and 1D). The desired band was cut from the gel and rehydrated in water (400 μl). After removal of the paper, the gel was crushed and the mixture was left to stand for 3 hr at room temperature. A solution of the PKIP-pore (T129C-D8-TEG-PKIP5-24$_1$WT$_6$) was obtained by removal of the polyacrylamide gel with a cellulose acetate filter (0.2 μm diameter; Rainin, Woburn, MA). αHL homoheptamer, WT_7, was made by the same method. The protein pores were stored at –80°C before they were used for planar bilayer recordings.

cAMP-Dependent Protein Kinase C Subunit

Wild-type mouse C_α subunit and the C343S mutant were gifts from Keyong Zou. The two enzymes have indistinguishable kinetic prop-

erties and were used interchangeably in this work. Both were purified after expression in *E. coli*. The low-mass thiols in the stored enzyme solutions were removed by passage through gel filtration spin columns (Sephadex G-25, Harvard Apparatus). With BSA as a standard, the final concentrations of the C subunits were determined with the Bio-Rad protein assay dye reagent (500-0006, Bio-Rad Laboratories, Hercules, CA). The specific catalytic activities of C_α and C343S were determined [50] and found to be 24 ± 1 and 23 ± 2 μmol min^{-1} mg^{-1}, respectively.

Planar Bilayer Recordings

Planar lipid membrane recordings were carried out at 25°C. The *cis* and *trans* chambers of the apparatus, each 1.5 ml, were separated by a 25 μm thick Teflon septum (Goodfellow Corporation, Malvern, PA). An aperture in the septum (~150 μm diameter) was pretreated with 10% (v/v) hexadecane (Aldrich) in *n*-pentane (Burdick and Jackson, Muskegon, MI). The electrolyte in both chambers was 300 mM KCl, 15 mM MOPS (pH 6.80). A bilayer membrane was formed with 1,2-diphytanoyl-*sn*-glycerophosphocholine (Avanti Polar Lipids, Alabaster, AL). αHL protein pores were introduced by adding the gel-purified heptamers (0.5 μl) to the *cis* side of the chamber, which was stirred until a single pore inserted (29 pA step at –100 mV).

Currents were recorded through Ag/AgCl electrodes by using a patch clamp amplifier (Dagan 3900A with the 3910 expander module; Dagan Corporation, Minneapolis, MN). The signal was filtered at 5 kHz with a four-pole internal Bessel filter and stored with a digital audio tape recorder (DAS-75). The *cis* chamber was held at ground, and a negative current (downward deflection) represents positive charge moving from the *cis* to the *trans* side. A Pentium PC equipped with a DigiData 1200 A/D converter (Axon Instruments, Foster City, CA) and the Fetchex program of pClamp 8 were used for data acquisition. For computer analysis, the data were further filtered with an eight-pole Bessel filter at frequencies in the range of 100–3000 Hz and sampled at 10 kHz.

Data Analysis

Single-Channel Current Recording

The data were analyzed and presented by using pClampfit 9.0 and Origin 6.0. Mean residence (dwell) time values (τ) were obtained from dwell-time histograms by fitting the distributions to exponential functions. Numerical data are given with standard deviations; n values refer to the number of independent experiments. In the single-channel experiments, the values of the association rate constant (k_{on}), dissociation rate constant (k_{off}), and equilibrium dissociation constant (K_d) for the C subunit were calculated based on τ_{on} (the interevent interval) and τ_{off} (the dwell time of C at the pore):

$$\frac{1}{\tau_{on}} = k_{on}[E], \frac{1}{\tau_{off}} = k_{off}, \text{ and } K_d = \frac{k_{off}}{k_{on}}$$

Macroscopic Current Recording

The decay of the current through about a hundred PKIP-pores in the presence of various concentrations of C subunit was recorded at 25 ± 1°C after a step from +100 mV to various negative applied potentials between –70 mV and –120 mV. The current decays were used to obtain values of k_{on} and k_{off} by modifying an approach described earlier [51] (see Supplemental Data).

Competition of C Subunit Binding with PKIP

Single-channel currents through the PKIP-pore were recorded in the presence of 150 nM C subunit in the absence and presence of free PKIP5-24 peptide (2 μM) in the *trans* chamber. The experiment was carried out at –80 mV at 25 ± 1°C.

Supplemental Data

Supplemental Data are available at http://www.chembiol.com/cgi/content/full/12/1/109/DC1/.

Acknowledgments

We thank Dr. Larry Dangott at the Protein Chemistry Laboratory in the Department of Biochemistry and Biophysics at Texas A&M University for his help in the characterization of peptide conjugates by MALDI-MS, Dr. Keyong Zou for providing C subunits of PKA, and the referees for helpful comments. Work at Texas A&M University was supported by DARPA, the DoD Tri-Service Technology Program, DOE, NASA, NIH, ONR, and the Welch Foundation. H.B. is the holder of a Royal Society-Wolfson Research Merit Award. O.B. is supported by the Wellcome Trust.

Received: September 11, 2004
Revised: November 4, 2004
Accepted: November 5, 2004
Published: January 21, 2005

References

1. Adams, J.A. (2001). Kinetic and catalytic mechanisms of protein kinases. Chem. Rev. *101*, 2271–2290.
2. Zhu, H., Klemic, J.F., Chang, S., Bertone, P., Casamayor, A., Klemic, K.G., Smith, D., Reed, M.A., and Snyder, M. (2000). Analysis of yeast protein kinases using protein chips. Nat. Genet. *26*, 283–289.
3. Houseman, B.T., Huh, J.H., Kron, S.J., and Mrksich, M. (2002). Peptide chips for the quantitative evaluation of protein kinase activity. Nat. Biotechnol. *20*, 270–274.
4. Phizicky, E., Bastiaens, P.I., Zhu, H., Snyder, M., and Fields, S. (2003). Protein analysis on a proteomic scale. Nature *422*, 208–215.
5. Dunn, D.A. (2002). Mining the "human" kinome. Drug Discov. Today *7*, 1121–1123.
6. Noble, M.E.M., Endicott, J.A., and Johnson, L.N. (2004). Protein kinase inhibitors: insights into drug design from structure. Science *303*, 1800–1805.
7. Smith, C.M., Radzio-Andzelm, E., Akamine, P., and Taylor, S.S. (1999). The catalytic subunit of cAMP-dependent protein kinase: prototype for an extended network of communication. Prog. Biophys. Mol. Biol. *71*, 313–341.
8. Johnson, D.A., Akamine, P., Radzio-Andzelm, E., and Taylor, S.S. (2001). Dynamics of cAMP-dependent protein kinase. Chem. Rev. *101*, 2243–2270.
9. Manning, G., Whyte, D.B., Martinez, R., Hunter, T., and Sudarsanam, S. (2002). The protein kinase complement of the human genome. Science *298*, 1912–1934.
10. Knighton, D.R., Zheng, J., Ten Eyck, L.F., Xuong, N.-H., Taylor, S.S., and Sowadski, J.M. (1991). Crystal structure of the catalytic subunit of cyclic adenosine monophosphate-dependent protein kinase. Science *253*, 407–414.
11. Engh, R.A., Girod, A., Kinzel, V., Huber, R., and Bossemeyer, D. (1996). Crystal structures of catalytic subunit of cAMP-dependent protein kinase in complex with isoquinolinesulfonyl protein kinase inhibitors H7, H8, and H89. J. Biol. Chem. *271*, 26157–26164.
12. Akamine, P., Xuong, N.H., and Taylor, S.S. (2002). Crystal structure of a transition state mimic of the catalytic subunit of cAMP-dependent protein kinase. Nat. Struct. Biol. *9*, 273–277.
13. Yang, J., Ten Eyck, L.F., Xuong, N.H., and Taylor, S.S. (2004). Crystal structure of a cAMP-dependent protein kinase mutant at 1.26Å: new insights into the catalytic mechanism. J. Mol. Biol. *336*, 473–487.
14. Knighton, D.R., Zheng, J., Ten Eyck, L.F., Xuong, N.-H., Taylor, S.S., and Sowadski, J.M. (1991). Structure of a peptide inhibitor bound to the catalytic subunit of cyclic adenosine monophosphate-dependent protein kinase. Science *253*, 414–420.
15. Bayley, H., and Cremer, P.S. (2001). Stochastic sensors inspired by biology. Nature *413*, 226–230.
16. Movileanu, L., Howorka, S., Braha, O., and Bayley, H. (2000). Detecting protein analytes that modulate transmembrane movement of a polymer chain within a single protein pore. Nat. Biotechnol. *18*, 1091–1095.
17. Howorka, S., Nam, J., Bayley, H., and Kahne, D. (2004). Stochastic detection of monovalent and bivalent protein-ligand interactions. Angew. Chem. Int. Ed. Engl. *43*, 842–846.
18. Song, L., Hobaugh, M.R., Shustak, C., Cheley, S., Bayley, H., and Gouaux, J.E. (1996). Structure of staphylococcal α-hemo-

lysin, a heptameric transmembrane pore. Science *274*, 1859–1865.
19. Kramer, R.H., and Karpen, J.W. (1998). Spanning binding sites on allosteric proteins with polymer-linked ligand dimers. Nature *395*, 710–713.
20. Blaustein, R.O., Cole, P.A., Williams, C., and Miller, C. (2000). Tethered blockers as molecular 'tape measures' for a voltage-gated K^+ channel. Nat. Struct. Biol. *7*, 309–311.
21. Scott, J.D., Fischer, E.H., Demaille, J.G., and Krebs, E.G. (1985). Identification of an inhibitory region of the heat-stable protein inhibitor of the cAMP-dependent protein kinase. Proc. Natl. Acad. Sci. USA *82*, 4379–4383.
22. Scott, J.D., Glaccum, M.B., Fischer, E.H., and Krebs, E.G. (1986). Primary structure requirements for inhibition by the heat-stable inhibitor of the cAMP-dependent protein kinase. Proc. Natl. Acad. Sci. USA *83*, 1613–1616.
23. Glass, D.B., Cheng, H.C., Kemp, B.E., and Walsh, D.A. (1986). Differential and common recognition of the catalytic site of the cGMP-dependent and cAMP-dependent protein kinases by inhibitory peptides derive from the heat-stable inhibitor protein. J. Biol. Chem. *261*, 12166–12171.
24. Herberg, F.W., and Taylor, S.S. (1993). Physiological inhibitors of the catalytic subunit of cAMP-dependent protein kinase: effect of MgATP on protein-protein interaction. Biochemistry *32*, 14015–14022.
25. Hauer, J.A., Barthe, P., Taylor, S.S., Parello, J., and Padilla, A. (1999). Two well-defined motifs in the cAMP-dependent protein kinase inhibitor (PKIa) correlate with inhibitory and nuclear export function. Protein Sci. *8*, 545–553.
26. Howorka, S., Cheley, S., and Bayley, H. (2001). Sequence-specific detection of individual DNA strands using engineered nanopores. Nat. Biotechnol. *19*, 636–639.
27. Moczydlowski, E. (1986). Single-channel enzymology. In Ion Channel Reconstitution,, C. Miller, ed. (New York: Plenum Press), pp. 75–113.
28. Gu, L.-Q., Cheley, S., and Bayley, H. (2001). Prolonged residence time of a noncovalent molecular adapter, β-cyclodextrin, within the lumen of mutant α-hemolysin pores. J. Gen. Physiol. *118*, 481–494.
29. Bossemeyer, D., Engh, R.A., Kinzel, V., Postingl, H., and Huber, R. (1993). Phosphotransferase and substrate binding mechanism of the cAMP-dependent protein kinase catalytic subunit from porcine heart as deduced from the 2.0 Å structure of the complex with Mn^{2+} adenylyl imidodiphosphate and inhibitor peptide PKI(5–24). EMBO J. *12*, 849–859.
30. Whitehouse, S., and Walsh, D.A. (1983). $Mg{\bullet}ATP^{2-}$ dependent interaction of the inhibitor protein of the cAMP-dependent protein kinase with the catalytic subunit. J. Biol. Chem. *258*, 3682–3692.
31. Lew, J., Coruh, N., Tsigelny, I., Garrod, S., and Taylor, S.S. (1997). Synergistic binding of nucleotides and inhibitors to cAMP-dependent protein kinase examined by acrylodan fluorescence spectroscopy. J. Biol. Chem. *272*, 1507–1513.
32. Trafny, E.A., Xuong, N.H., Adams, J.A., Ten Eyck, L.F., Taylor, S.S., and Sowadski, J.M. (1994). cAMP-dependent protein kinase: crystallographic insights into substrate recognition and phosphotransfer. Protein Sci. *3*, 176–187.
33. Xie, X.S., and Lu, H.P. (1999). Single-molecule enzymology. J. Biol. Chem. *274*, 15967–15970.
34. Noji, H., and Yoshida, M. (2001). The rotary machine in the cell, ATP synthase. J. Biol. Chem. *276*, 1665–1668.
35. Ishijima, A., and Yanagida, T. (2001). Single molecule nanobioscience. Trends Biochem. Sci. *26*, 438–444.
36. Ishijima, A., Kojima, H., Funatsu, T., Tokunaga, M., Higuchi, H., Tanaka, H., and Yanagida, T. (1998). Simultaneous observation of individual ATPase and mechanical events by a single myosin molecule during interaction with actin. Cell *92*, 161–171.
37. Levene, M.J., Korlach, J., Turner, S.W., Foquet, M., Craighead, H.G., and Webb, W.W. (2003). Zero-mode waveguides for single-molecule analysis at high concentrations. Science *299*, 682–686.
38. Noji, H., Yasuda, R., Yoshida, M., and Kinosita, K. (1997). Direct observation of the rotation of F_1-ATPase. Nature *386*, 299–302.
39. Panchal, R.G., Cheley, S., and Bayley, H. (1994). Differential phosphorylation of neuronal substrates by catalytic subunits of *Aplysia* cAMP-dependent protein kinase with alternative N termini. J. Biol. Chem. *269*, 23722–23730.
40. Resh, M.D. (1994). Myristylation and palmitylation of src family members: the fats of the matter. Cell *76*, 411–413.
41. McLaughlin, S., and Aderem, A. (1995). The myristoyl-electrostatic switch: a modulator of reversible protein-membrane interactions. Trends Biochem. Sci. *20*, 272–276.
42. Murray, D., Hermida-Matsumoto, L., Buser, C.A., Tsang, J., Sigal, C.T., Ben-Tal, N., Honig, B., Resh, M.D., and McLaughlin, S. (1998). Electrostatics and the membrane association of Src: theory and experiment. Biochemistry *37*, 2145–2159.
43. Liang, X., Lu, Y., Wilkes, M., Neubert, T.A., and Resh, M.D. (2004). The N-terminal SH4 region of the Src family kinase Fyn is modified by methylation and heterogeneous fatty acylation: role in membrane targeting, cell adhesion, and spreading. J. Biol. Chem. *279*, 8133–8139.
44. Carnegie, G.K., and Scott, J.D. (2003). A-kinase anchoring proteins and neuronal signaling mechanisms. Genes Dev. *17*, 1557–1568.
45. Holmes, T.C., Berman, K., Swartz, J.E., Dagan, D., and Levitan, I.B. (1997). Expression of voltage-gated potassium channels decreases cellular protein tyrosine phosphorylation. J. Neurosci. *17*, 8964–8974.
46. Oliver, D., Lien, C.-C., Soom, M., Baukrowitz, T., Jonas, P., and Fakler, B. (2004). Functional conversion between A-type and delayed rectifier K^+ channels by membrane lipids. Science *304*, 265–270.
47. Tegge, W., Frank, R., Hofmann, F., and Dostmann, W.R.G. (1995). Determination of cyclic nucleotide-dependent protein kinase substrate specificity by the use of peptide libraries on cellulose paper. Biochemistry *34*, 10569–10577.
48. Braunwalder, A.F., Yarwood, D.R., Hall, T., Missbach, M., Lipson, K.E., and Sills, M.A. (1996). A solid-phase assay for the determination of protein tyrosine kinase activity of c-src using scintillating microtitration plates. Anal. Biochem. *234*, 23–26.
49. Carlsson, J., Drevin, H., and Axen, R. (1978). Protein thiolation and reversible protein-protein conjugation. N-succinimidyl 3-(2-pyridyldithio)propionate, a new heterobifunctional reagent. Biochem. J. *173*, 723–737.
50. Zou, K., Cheley, S., Givens, R.S., and Bayley, H. (2002). Catalytic subunit of protein kinase A caged at the activating phosphothreonine. J. Am. Chem. Soc. *124*, 8220–8229.
51. Cheley, S., Gu, L.-Q., and Bayley, H. (2002). Stochastic sensing of nanomolar inositol 1,4,5-trisphosphate with an engineered pore. Chem. Biol. *9*, 829–838.
52. Zimmermann, B., Chiorini, J.A., Ma, Y., Kotin, R.M., and Herberg, F.W. (1999). PrKX is a novel catalytic subunit of the cAMP-dependent protein kinase regulated by the regulatory subunit type I. J. Biol. Chem. *274*, 5370–5378.